

**PHOTOMETRY OF LUNAR LANDING SITES USING LROC NAC IMAGES AND HAPKE MODELING.**

R. N. Clegg<sup>1</sup>, B. L. Jolliff<sup>1</sup>, M. S. Robinson<sup>2</sup>, B. W. Hapke<sup>3</sup>, and J. B. Plescia<sup>4</sup>, <sup>1</sup>Dept. of Earth and Planetary Sciences, Washington University in St. Louis, 1 Brookings Dr., St. Louis, MO 63130, [rclegg@levee.wustl.edu](mailto:rclegg@levee.wustl.edu), <sup>2</sup>School of Earth and Space Exploration, Arizona State University, Tempe, AZ, <sup>3</sup>Dept. of Geology and Planetary Science, University of Pittsburgh, Pittsburgh, PA, <sup>4</sup>Applied Physics Lab, Johns Hopkins University, Baltimore, MD.

**Introduction:** Lunar Reconnaissance Orbiter Camera (LROC) Narrow Angle Camera (NAC) images show areas of increased reflectance around the Apollo, Luna, and Surveyor landing sites. These areas are interpreted as regions that have been disturbed by rocket exhaust and are referred to as “blast zones” (BZs) [1,2]. The BZs consist of an area of lower reflectance (LR-BZ) compared to the surroundings that extends up to a few meters out from the landers and a broader halo of higher reflectance (HR-BZ) that extends tens to hundreds of meters out from the landers.

We use phase-ratio images [1,2], reflectance profiles, and Hapke photometric modeling of NAC image data collected over a range of illumination geometries, as well as surface photos (Apollo) and descriptions and compositions of soil samples to investigate what physical properties of the regolith changed to create an increase in reflectance within the HR-BZs and a decrease within the LR-BZs. We have been testing the following possible explanations for the reflectance changes: 1) change in macroscopic roughness (cm to m scale), 2) redistribution of fine particles (excavation from LR-BZ and deposition to HR-BZ), 3) removal of a more mature surface layer and exposure of less mature soil, 4) microscopic (nm to  $\mu\text{m}$  scale) modification of fine-scale structure (e.g., “fairy castle” structure, see [3]), 5) compaction of the regolith within the more reflective area, 6) contamination from rocket fuel, or 7) some combination of these effects.

**Methods:** Phase-ratio images are created using NAC images and provide enhanced contrast between the disturbed and undisturbed regions. They have proven very effective in measuring the spatial extent of the BZs. Reflectance profiles taken across the landing site give quantitative information on how reflectance ( $I/F$ ) changes within the HR-BZ, the LR-BZ, and in background regions, i.e., areas unaffected by rocket exhaust. They also serve as a confirmation of the spatial extents of the BZs.

**Hapke Photometric Modeling:** The goals of photometric modeling are to test variable parameters to determine which could best account for the reflectance characteristics we see over a range of illumination conditions [4,5]. We fit the NAC reflectance data using the Hapke simplified bidirectional reflectance function [6,7], which is the ratio of the radiance  $I$  received at the detector viewing the surface from angle  $e$  to the radiance  $F$  from the source at angle  $i$ , and then normalizing to the Lommel-Seeliger Function (LS):

$$(1) \quad \frac{IoF}{LS} = \frac{w}{4} [p(g) + H(\mu_0, w)H(\mu, w) - 1] [1 + B_{c0}B_c(g, h_c)] S(i, e, \theta)$$

$$(2) \quad LS = \mu_0 / (\mu_0 + \mu)$$

where parameters are defined in [6] and [7] and dividing by the Lommel-Seeliger function masks some of the effects of viewing geometry [7]. The single scattering albedo ( $w$ ) is dependent on properties such as composition and grain size, and varies for each landing site. We hold  $w$  constant across the HR-BZ and background at each site, but vary the mean slope angle,  $\theta$ , in order to fit the observed reflectance data. The mean slope angle is related to roughness, so varying this parameter reveals differences in roughness between the HR-BZ and background. We use a double Henyey-Greenstein function [7] for  $p(g)$  and vary the  $b$  parameter inherent within this function, which is dependent on grain size.

**Results: Blast Zone Spatial Extents:** When approximated as an ellipse, the average Apollo BZ area is  $\sim 29,000 \text{ m}^2$  ( $\sim 175 \pm 60 \text{ m}$  by  $200 \pm 27 \text{ m}$ ) which is 10x larger than the average Luna BZ, and over 100x larger than the average Surveyor BZ (Table 1). The BZ area scales non-linearly as a function of lander thrust. The Luna 24 BZ is anomalous (see [8]) and is not included in our statistical analysis.

**Photometry:** The LR-BZs are most evident at the Apollo sites, especially where astronaut activity has roughed up the soil, leading to a 2-14% reduction in reflectance at  $\sim 30^\circ$  phase angle. The LR-BZs at the Surveyor and Luna sites are less evident and appear to be confined to the area below the landers. The average normalized reflectance (HR-BZ reflectance normalized to background reflectance) in the HR-BZs for images with a  $\sim 30^\circ$  phase angle is 10-16% higher on average than in the undisturbed surrounding areas; this magnitude is the same, within uncertainty, for all sites, indicating a common process or combination of processes cause the differences in reflectance properties of the

Table 1: Average reflectance values and area measurements for the lunar landing sites. Normalized  $I/F = IoF(\text{HR-BZ})/IoF(\text{bckgrnd})$ .

Mission	Avg. normalized I/F	Avg. elliptical area ( $\text{m}^2$ )	Avg. thrust (kN)
Apollo	1.143	28785	45
Luna	1.106	2380	15-20
Surveyor	1.156	215	0.133-0.472

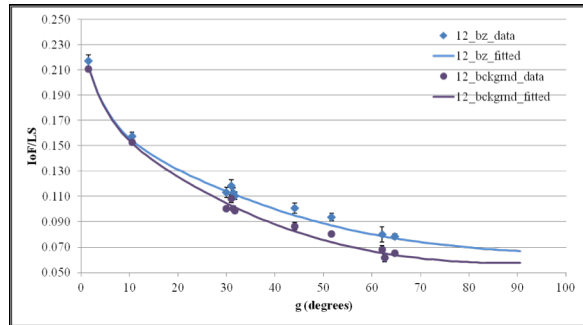


Figure 1: Apollo 12 HR-BZ and background reflectance data, fitted using Equation 1.

Table 2: Parameters for fitting Apollo 12 data

	$w$	$B_{co}$	$h_c$	$b$	$c$	$\theta$
<b>HR-BZ</b>	0.305	0.77	0.107	0.35	-0.20	2°
<b>Bckgrnd</b>	0.305	0.77	0.107	0.40	-0.20	25°

regolith. Phase-ratio images and photometric data collected over a range of illumination geometries show that a greater separation in  $I/F$  occurs between the HR-BZs and undisturbed areas with increasing phase angle and indicate that the HR-BZs are less backscattering than undisturbed areas. The reduction in backscattering characteristics is consistent with destruction of the fairy-castle structure within the BZs and the increased separation between BZ and background values at high phase is therefore likely due to smoothing within the HR-BZs.

**Hapke Photometric Modeling:** Figure 1 shows the Apollo 12 HR-BZ and background reflectance data, fitted using Equation (1). The parameters used are shown in Table 2. The mean slope angle is much lower within the HR-BZ than in the background, indicating the surface is less rough within the HR-BZ. We interpret this as macroscopic smoothing due to interaction of rocket exhaust with small-scale topography within the HR-BZ. This decrease in  $\theta$  within the HR-BZ is consistent across all of the Apollo and Luna landing sites.

**Compositional Effects:** We expect that the single scattering albedo should be closely related to composition at the landing sites. We have examined published compositional data [9-12] for  $\text{TiO}_2$ ,  $\text{Al}_2\text{O}_3$ , and  $\text{FeO}$  contents for various samples taken within and outside the BZs. Figure 2 shows a plot of  $\text{Al}_2\text{O}_3$  versus the modeled  $w$  for each of the Apollo and Luna landing sites. The correlation between  $w$  and  $\text{Al}_2\text{O}_3$  is very good ( $R^2=0.91$ ), and  $w$  increases as  $\text{Al}_2\text{O}_3$  content increases. This trend is expected, since  $\text{Al}_2\text{O}_3$  correlates inversely with  $\text{FeO}$ . The sample with the lowest  $\text{Al}_2\text{O}_3$ , Luna 24, is immature and may not be representative of the surface regolith. The two sites with the highest  $\text{Al}_2\text{O}_3$  content, Apollo 16 and Luna 20, are the two sites that landed in the highlands; they have the highest

$\text{Al}_2\text{O}_3$  and plagioclase content and therefore the highest  $w$ . Holding  $w$  constant and changing  $\theta$  for the HR-BZ and background data sets provides the best model fit.

**Conclusions:** On the basis of Hapke photometric modeling and examination of the phase-ratio images, we infer that the increased reflectance within the HR-BZs is best explained by destruction of the fine-scale structure and smoothing of the regolith. Decreased values of  $\theta$  for the Hapke fits for all sites indicate that macroscopic roughness changes occurred within the HR-BZs. These conclusions are consistent with those of Kaydash et al. [1] and Shkuratov et al. [8]. The modeled  $w$  values behave as expected – increasing with increasing  $\text{Al}_2\text{O}_3$  content – and model fits are best when  $w$  is held constant for the HR-BZ and background at each site. The varying values of  $b$  may be related to grain size changes, but plume effects modeling does not seem to support this so we will be investigating the redistribution of fine particles hypothesis in future studies. Exposure of less mature soil is unlikely because exhaust plumes did not excavate to depths large enough to expose sufficiently less mature soil [13-15]. The decreased reflectance within the LR-BZs was caused by clumping and pitting of the soil beneath the rocket nozzle, and enlarged by astronaut activity roughing up the surface [16].

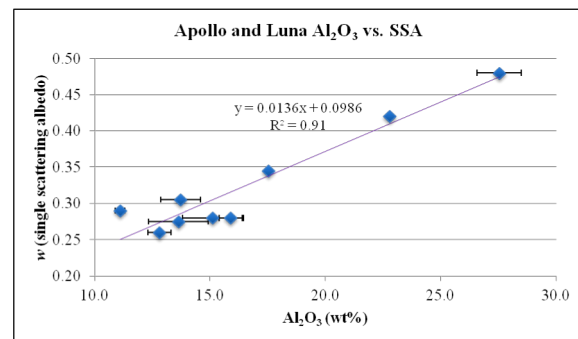


Figure 2: Single scattering albedo values used for modeling as a function of  $\text{Al}_2\text{O}_3$  content for the Apollo and Luna landing sites. Errors calculated using data from [10,15].

**Acknowledgements:** We thank the LROC Operations Team for image collection and processing, and the science team for much help. We thank NASA for support of the LRO mission.

**References:** [1] Kaydash V. et al. (2011), *Icarus*, 211, 89-96. [2] Clegg R. N. and Jolliff B. L. (2012), *LPSC XLIII*, Abstract #2030. [3] Hapke B. and van Horn H. (1963), *JGR*, 68, 4545. [4] Hapke B.W. (1981), *JGR*, 86, 3039-54. [5] Carrier W.D. (1991), *Lunar Sourcebook*, 475-594. [6] Hapke B. W. (2001), *Icarus*, 167, 523-524. [7] Hapke B. W. et al. (2012), *JGR*, 117. [8] Shkuratov Y. et al. (2012), *PSS*, E00115. [9] Graf J. (1993), *Lunar Soils Grain Size Catalog*. [10] Morris R. V. et al. (1983), *Handbook of Lunar Soils*. [11] Blanchard, D. P. et al. (1977), *LPI Conference on Luna 24*. [12] Laul, J. C., and Schmitt E. A. (1973), *GCA*, 37, 927-942. [13] Kaydash V. G. and Shkuratov Y. G. (2012), *SSR*, 46, 108-118. [14] Immer C. et al. (2011), *Icarus*, 211, 1089-1102. [15] Lucey, P. et al. (2006), *New Views of the Moon*, 84-219. [16] Hapke B. W. (1972), *Moon*, 3, 456-460.